Discrete simulations of spatio-temporal dynamics of small water bodies under varied stream flow discharges

B. S. Daya Sagar

Nonlinear Processes in Geophysics (2005) 12: 31–40
SRef-ID: 1607-7946/npg/2005-12-31
European Geosciences Union

Nonlinear Processes in Geophysics

Discrete simulations of spatio-temporal dynamics of small water bodies under varied stream flow discharges

B. S. Daya Sagar

Faculty of Engineering and Technology, Melaka Campus, Multimedia University, Jalan Ayer Keroh Lama, 75450, Melaka, Malaysia

Received: 12 May 2004 – Revised: 16 November 2004 – Accepted: 17 November 2004 – Published: 17 January 2005

Part of Special Issue "Nonlinear deterministic dynamics in hydrologic systems: present activities and future challenges"

Abstract. Spatio-temporal patterns of small water bodies (SWBs) under the influence of temporally varied stream flow discharge are simulated in discrete space by employing geomorphologically realistic expansion and contraction transformations. Cascades of expansion-contraction are systematically performed by synchronizing them with stream flow discharge simulated via the logistic map. Templates with definite characteristic information are defined from stream flow discharge pattern as the basis to model the spatio-temporal organization of randomly situated surface water bodies of various sizes and shapes. These spatio-temporal patterns under varied parameters (λs) controlling stream flow discharge patterns are characterized by estimating their fractal dimensions. At various λs, nonlinear control parameters, we show the union of boundaries of water bodies that traverse the water body and non-water body spaces as geomorphic attractors. The computed fractal dimensions of these attractors are 1.58, 1.53, 1.78, 1.76, 1.84, and 1.90, respectively, at λs of 1, 2, 3, 3.46, 3.57, and 3.99. These values are in line with general visual observations.

1 Introduction

Flood plain is found in an area of ecological transition from wet to dry and is characterized by flood and low water regimes. Flood and drought are two extreme events that show impact on climatically sensitive small water bodies (SWBs). Flood and drought are the effects, respectively, due to stream flow discharge that is more or less than mean stream flow discharge (MSD). Stream flow discharge dynamics control the morphological dynamics of ephemeral SWBs that exist within a basin with less relief ratio, as there would not be much difference between the highest and lowest observed elevations in the floodplain basins. Due to this low relief ratio, the expansions and contractions of SWBs under the influence of variations in the stream flow discharge pattern are assumed isotropic. They tend to merge with each other during peak stream flow discharge much larger than MSD. In contrast, due to intense drought during which the stream flow discharge is much lesser than MSD, the spatio-temporal organization of water bodies will be disturbed.

The homogeneous and heterogeneous progressive and retrogressive growths of lakes depend on various physical, meteorological, and physiographic factors. In a single dynamical system, these two phases may occur successively under the influence of peak-stream flow discharge followed by low-stream flow discharge that, respectively, lead to flood and drought. The homogeneous the stream flow discharge behavioral pattern, the more is the predictability of morphological dynamics of SWBs. The heterogeneous is the stream flow discharge over a time period, the more complex is the morphological evolution.

In general, varied degrees of two types of morphological changes that we visualize include isotropic expansion and contraction. This investigation is based on the following postulates: (i) variations in stream flow discharge pattern cause modifications in geomorphic organization; (ii) expansion and contraction depend on original spatial organization, as sparser phenomenon is worst affected due to low stream flow discharge compared to denser phenomena; and (iii) morphological evolutionary pattern in these phenomena follows the stream flow discharge behavioral pattern. The heterogeneities in these morphological processes may be attributed to topographic effects.

It is reported in several studies that the behavior of such stream flow discharges may produce low dimensional attractor that depicts chaoticity (e.g. Savard, 1990, 1992; Tsonis et al., 1994; Jayawardena and Lai, 1994; Beauvais and Dubois, 1995; Pasternack, 1999; Sivakumar, 2004). In these studies, correlation dimension of attractors governing the trajectories of stream flow discharge dynamics describe the degree of chaoticity in the stream flow discharge time series. In the present investigation, time series of such mean discharges are simulated through first order nonlinear difference equa-

Correspondence to: B. S. Daya Sagar
(bsdaya.sagar@mmu.edu.my)

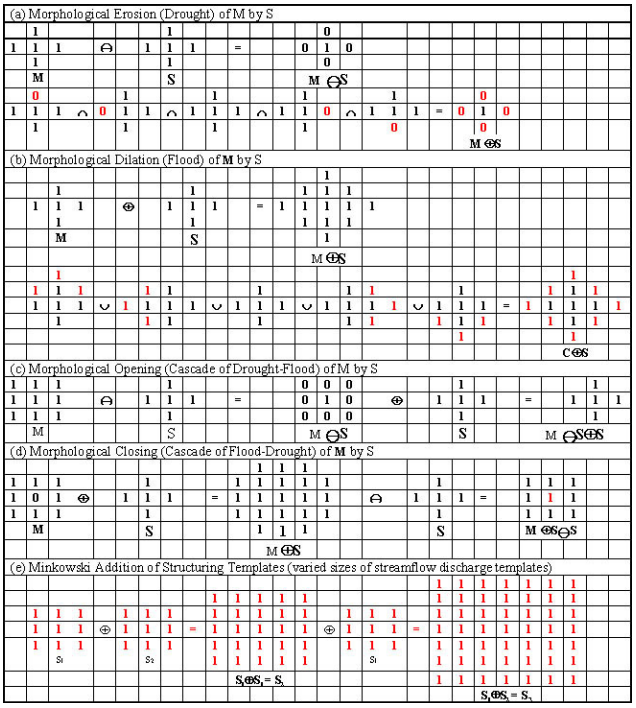

Fig. 1. Mathematical morphological transformations and their matrix representations: **(a)** erosion (drought) and **(b)** dilation (flood) by means of a template (stream flow discharge template) that is rhombus in shape, 3×3 in size with center as origin, **(c)** opening (cascade of drought-flood) and **(d)** closing (cascade of flood-drought) by means of rhombus template, and **(e)** structuring templates (stream flow discharge templates) of different sizes that are created via Minkowski's addition. Two templates (S_1) of size 3×3 becomes 5×5 (S_2), and $S_1 \oplus S_2$ yields a larger template of size 7×7 (S_3).

tion, the logistic map, further to relate the impact of changing stream flow discharges on spatio-temporal organization of randomly situated SWBs.

Although this study, on simulation of morphological dynamics of SWBs by employing mathematical morphological transformations, is first of its kind, the applications of morphological transformations in the context of geomorphology and geophysics are common in extraction of significant geomorphologic features from digital elevation models (Sagar, 2001; Sagar et al., 2001, 2003; Chockalingam and Sagar, 2003), estimation of basic measures of water bodies (Sagar et al., 1995a, b) and roughness indexes of terrain (Tay et al., 2004[1]), modeling and simulation of geomorphic processes (Sagar et al., 1998; Sagar, 2001), generation of fractal landscapes (Sagar and Murthy, 2000), and fractal relationships among various parameters of geomorphologic interest (Sagar and Rao, 1995; Sagar, 1996, 1999, 2000; Sagar et al., 1998, 1999, 2001; Sagar and Tien, 2004; Sagar and Chockalingam, 2004; Chockalingam and Sagar, 2004[2]).

[1]Tay, L. T., Sagar, B. S. D., and Chuah, H. T.: Derivation of terrain roughness indicators via Granulometries, Geophys. Res. Lett., under review, 2004.

[2]Chockalingam, L. and Sagar, B. S. D.: Morphometry of networks and non-network spaces, J. Geophys. Res., under review, 2004.; Tay et al., 2004.

Large floods and intense droughts are capable of inducing spectacular changes in the morphological configuration of water body and its surroundings. Multi-date earth observing remotely sensed satellite data of various resolutions are of use to monitor the climatically sensitive SWBs (e.g. Harris, 1994). Hitherto, many studies emphasize characterizing the time series of one-dimensional stream flow discharge data to understand its behavioral pattern. The impacts of varied types of such patterns on the spatial phenomena (e.g. water bodies, streams) can be observed via two-dimensional maps retrieved from various remotely sensing sources at temporal intervals. By considering the SWBs that could be precisely retrieved from multi-date remotely sensed data, one can understand the spatio-temporal organization of the climatically sensitive SWBs to further validate the theoretical discrete models. The changes in planar shapes and sizes of climatically sensitive lakes can be better mapped from multi-date remotely sensed satellite data. These changes can be spatially correlated with the changes in stream flow discharge pattern. Towards this direction, this paper gives a new insight to investigations, by stressing the importance of the geometry and topology of the randomly distributed SWBs.

What follows includes the procedures to simulate flood and drought via geomorphologically realistic mathematical morphological transformations, and to derive unique connectivity networks in Sect. 2. In Sect. 3, a sample study describing a morphology based scheme to show an interplay between numerical stream flow discharges simulated through first order difference equation, the logistic map, and their impacts on the small water body morphological dynamics, and followed by discussion on the results in Sect. 4. Conclusions with scope for further research are provided in Sect. 5.

2 Expansion-contraction due to flood-drought

During progressive and retrogressive growths, SWBs, respectively, flood and vanish or disintegrate and then vanish. These two processes are simulated under the influence of various stream flow discharge behavioral patterns in discrete space by employing geomorphologically realistic expansion and shrinking transformations. These transformations of varied degrees are termed as the two succeeding phases of a geomorphic system. These transformations are popularly known as "dilation" and "erosion" (Matheron, 1975; Serra, 1982), hereafter referred to as flood and drought transformations. To better understand the flood and drought transformations due to variations in the amount of stream flow discharge, we first introduce morphological erosion (drought) (Fig. 1a) and dilation (flood) (Fig. 1b), by means of a template (stream flow discharge).

Let M be a section consisting of binary water bodies (e.g. Fig. 2), where the pixels with 1s represent water-body points. A template (S) (Fig. 1e) in eight-connectivity grid, in which a point has eight neighbors, is considered. Template S is

moved from top to bottom and left to right by applying the criterion of either drought or flooding principle to, respectively, achieve drought or flood.

The "drought" transformation of M due to S is defined as the set of points m such that the translated S_m is contained in M and is expressed as:

$$M \ominus S = \{m : S_m \subseteq M\} = \cap_{s \in S} M_s. \quad (1)$$

The diagrammatic representation of implementation of drought transformation with the translates of all the elements of M by S is shown in Fig. 1a.

"Flood" is defined as a transformation that combines M and S using vector addition of set elements m and s, respectively, with m=(m_1,..., m_N) and s=(s_1, ..., s_N) being N-tuples of element co-ordinates. Then the flood of M by S is the set of all possible vector sums of pairs of elements, one coming from M and the other from S. The flood of M by S is defined as the set of all points m such that all translates of m by $s(S_m)$ intersects M, given by:

$$M \oplus S = \{m : S_m \cap M\} = \cup_{s \in S} M_s. \quad (2)$$

Figure 1b illustrates this transformation with possible translates of m by s, the union of which yields an expanded version of M. In both flood and drought transformations $-S$=$\{-s : s \in S\}$, i.e. S rotated 180° about the origin.

The neighboring water bodies are connected under continuous flood process, and the clustered water bodies are disconnected during continuous drought process. Water bodies merge together during the process of continuous expansion by incessant stream flow discharge. During the process of continuous contraction by S of size more than that of water body, the water body either disappears or first disintegrates and then disappears. To generate higher degrees of drought or flood, these transformation processes are iterated. Instead of using a larger S (for peak stream flow discharge), with the use of smaller S repeatedly, one will get the same effect. The cumulative S,of which the diagrammatic representation is shown in Fig. 1e, is mathematically represented as

$$S \oplus S \oplus S \oplus ... \oplus S = S_n. \quad (3)$$

Consecutive drought and flood transformations for n times are, respectively, represented as $(M \ominus S_n)$ and $(M \oplus S_n)$. The role of S that functions as an interface between water body and stream flow discharge is to simulate the effects of flood and drought. Figure 2 illustrates the continuous expansion of water bodies represented with clusters of 1's by means of S_1, S_2, and S_3. For better legibility, square templates with increasing size are employed to illustrate the effects of varied degrees of flood transformation. However, one can consider templates of asymmetric type with reference to origin to unravel other possible spatio-temporal patterns of small water bodies, in which the boundaries of dynamically changing water bodies may not be as uniform as we show in our results here. Various degrees of water body contractions or expansions can be simulated in discrete space by employing the hitherto explained transformations to understand the water

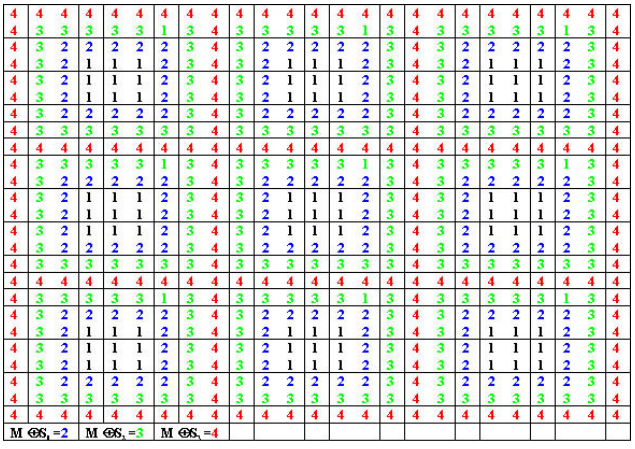

Fig. 2. Simulation of the impact due to flood transformation of three different intensities due to different degrees of stream flow discharges represented as (S_1), $(S_1 \oplus S_1)$=(S_2), and $S_1 \oplus S_2 = S_3$. Water bodies with clusters of digits 1's represent the water bodies at their stable state. The digits with 2's, 3's, and 4's, respectively, represent the impacts due to flood transformation with reference to S_1, S_2, and S_3. Three levels of flood propagating fronts are required to have flood-extinguishing pattern shown with digit 4's. Flood propagation shown here in a simulated manner is uniform.

body dynamical behavior under varied stream flow discharge patterns in discrete space.

The study of non-homogeneous nature of these cascade processes sheds light on the dynamical process in the natural water body evolution. During C-DF process (Fig. 1c), there is a possibility for the water body to either disappear or first disintegrate and then disappear. The effect of cumulative S,during the C-FD process (Fig. 1d) is represented as $(M \oplus S_n) \ominus S_n$. The characteristics of the S are assumed to be identical from one cycle to another in these two types of cascade processes. The characteristic information such as shape, size, origin, and orientation of this template (Fig. 1e), defined here as an entity due to which morphological changes occur in a water body, is important to simulate these processes in desired form, direction, and scale. Change in any of the characteristics of S during the sub-processes play major role in water body morphological transformations. For instance, for the cycle of water body evolution process from low-stream flow discharge period to peak stream flow discharge period to low-stream flow discharge period, the ensuing process is C-FD. The reverse process, visualized as periodic phases peak stream flow discharge period to low-stream flow discharge period to peak stream flow discharge period is C-DF.

2.1 Unique connectivity networks

Two unique connectivity networks include Flow Direction Network (*FDN*) and Self-organized Critical Connectivity Network Map (*SOCCNM*), which are one pixel wide caricatures that summarize the overall shape, size, orientation, and association of regions, respectively, occupied by water bodies (M) and their complementary space (M^c). The *FDN*

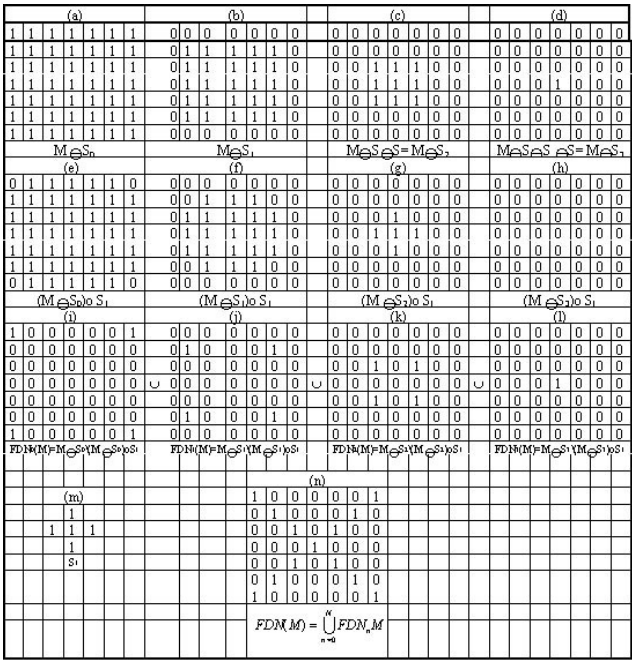

Fig. 3. Sequential steps involved in the extraction of flow direction network from a water body of size 7×7 represented with 1's. Sequential steps involved in isolation of various orders of FDN subsets is shown in this illustration: **(a)** discrete water body of size 7×7 pixels, **(b)–(h)** water body after iterative erosions (drought), **(i)–(l)** isolated FDN subsets of various degrees, **(m)** template used to perform iterative erosions shown in (b)–(h), and **(n)** union of FDN subsets of all degrees that produce FDN of water body shown in (a).

is mathematically defined as

$$FDN_n(M) = (M \ominus S_n)/\{[(M \ominus S_n) \ominus S_1] \oplus S_1,$$
$$n = 0, 1, 2, ..., N, \quad (4)$$

where $FDN_n(M)$ denotes the nth *FDN* subset of M. In the above expression, subtracting from the contracted versions of M their C-FD by S retains only the angular points. The union of all such possible points produces *FDN* within a water body (Fig. 3n). The sequential steps to extract *FDN* of M are illustrated in Fig. 3. Similar steps are needed to perform on non-water body space (M^c) to extract *SOCCNM* of M. Flooding process, during which randomly situated surface water bodies of various sizes and shapes self organize, is simulated mathematically as high degree of flood intensity makes the distant water bodies contact together to achieve *SOCCNM* (Fig. 4). In a way, *SOCCNM* depicts the extinguishing points of self-organized water bodies at a critical state. These two topographically significant networks (Fig. 4b) enable the structural composition of water bodies and their complementary space. In the process of extraction of *SOCCNM* subsets of nth order from the section containing water bodies (M) and no-water body regions (M^c), the C-DF versions of each eroded version of M^c are subtracted from the corresponding eroded version, is shown mathematically

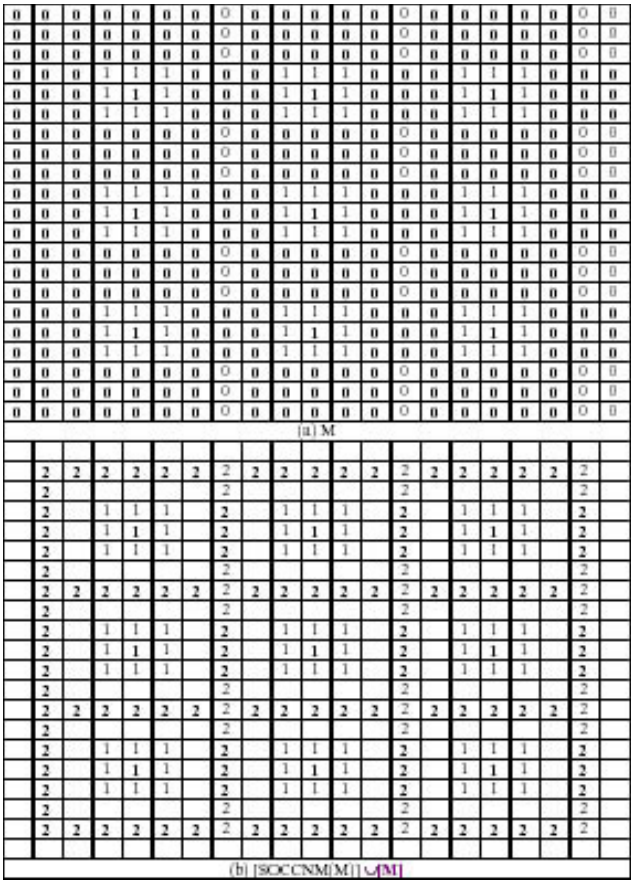

Fig. 4. (a) Section (M) containing nine equi-spaced discrete water bodies is represented with clusters of 1's. Their background space is represented with 0's, and **(b)** possible flow direction networks (FDNs) within these water bodies and a self-organized critical connectivity network map (SOCCNM) of section M are depicted, respectively, with 1's and 2's.

as

$$SOCCNM_n(M^c) = (M^c \ominus S_n)/\{[(M^c \ominus S_n) \ominus S] \oplus S. \quad (5)$$

Once, several orders of subsets of *FDN* and *SOCCNM* are isolated, respectively, from the water bodies and their complementary space, they are made union by following the logical AND operation as shown mathematically:

$$FDN(M) = \cup_{n=0}^{N} FDN_n(M) \quad (6)$$

$$SOCCNM(M) = \cup_{n=1}^{n} [SOCCNM_n(M^c)]. \quad (7)$$

Erosion and dilation mechanisms are employed to simulate the flood and drought impacts in discrete space. The importance of unique networks, the extraction of which is explained through equations, lies in the aspects of synchronizing the stream flow discharges with the travel time required for reaching the varied flood frontlines propagating from *FDN* to *SOCCNM*. The travel time is nothing but the size of the template. To simulate the effect of travel time in terms of the size of the template, we follow the postulate: A larger size of the template is required to simulate

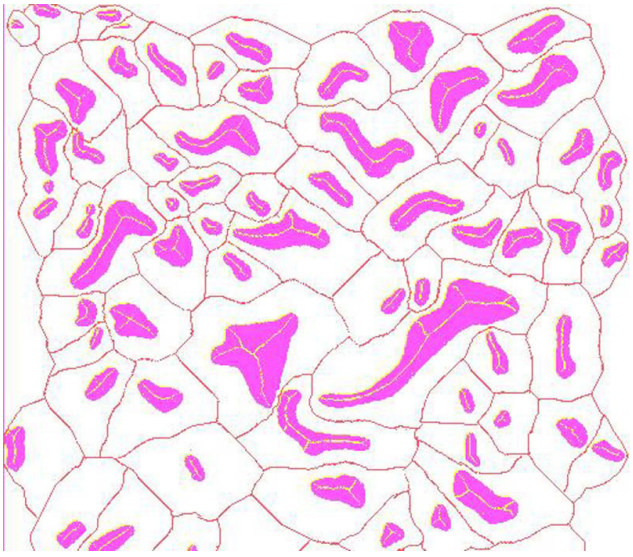

Fig. 5. Randomly distributed surface water bodies at their full capacity under the presence of MSD. Topological quantities FDN and SOCCNM are also shown.

a flood propagating at higher speed. However, we follow in this investigation that the propagation is uniform. These unique networks (e.g. Fig. 4b) such as *FDN* and *SOCCNM* are employed to derive a template with certain characteristic information to equate the stream flow discharges required to simulate complete flood and complete drought.

Diameter of S that is required to construct a large cell of *SOCCNM* from *FDN* is considered as $S_{\max}$ that makes all the SWBs merge. From Eqs. (6) and (7), S_N is defined as the template large enough to fill the largest cell achieved. The flood and drought transformations, and the transformations to extract *FDN*, and *SOCCNM*, are of use in visualizing all possible dynamical behaviors of SWBs under various stream flow discharge behavioral patterns.

3 Impact of stream flow discharge on spatial organization of SWBs: numeric vs. graphics

Patterns of orderly, periodically, and chaotically changing stream flow discharges at discrete time intervals are simulated through a first order nonlinear difference equation. By employing these patterns, simulations and computations are performed on a large number of randomly situated and climatically sensitive small water bodies (Fig. 5) of various sizes and shapes. These water bodies are from a flood plain region of the Gosthani River, one of east flowing rivers of India, within the geographical coordinates 18°07′ and 18°12′ north latitudes, and 83°17′ and 83°22′ east longitudes. These SWBs under respective cycles of contraction and expansion are shown in Figs. 6a and 6b, respectively, that depicts all possible frontlines from the origin to the *SOCCNM*.

We study the morphological evolution of these SWBs under the influence of various stream flow discharge inputs that

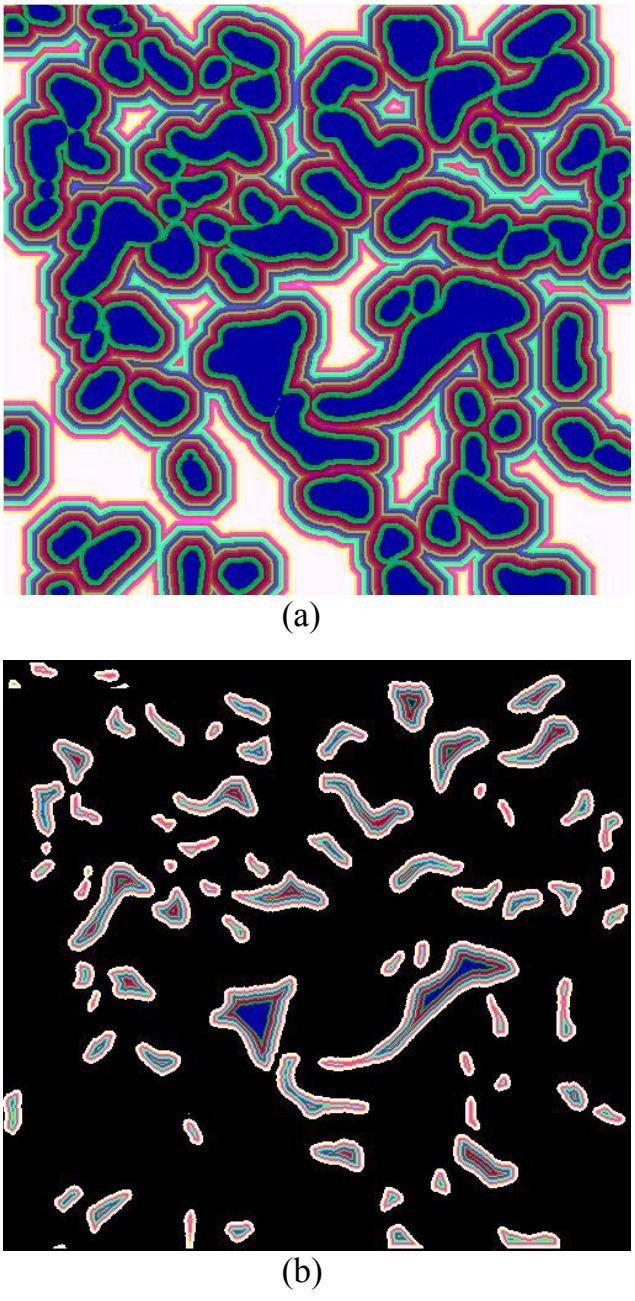

Fig. 6. (a) Water bodies under continuous flooding due to continuous peak stream flow discharge, and **(b)** drought due to low stream flow discharge input.

are simulated according to a first order difference equation (May, 1976) $A_{t+1}=\lambda A_t\,(1-A_t)$, where λ is environmental parameter $0\leq\lambda\leq4$, $0\leq A_t\leq1$; $A_t(t\to\infty)\to0$. The idea of considering this equation is that it can simulate several possible behaviors ranging from periodic, quasi-periodic to chaotic of various physical systems. Stream flow discharge in the normalized scale ranges from 0 to 1. It is shown that for $1\leq\lambda\leq3$ as $A_t(t\to\infty)\to$ constant value, the discharge value reaches a stable state and remains there. The environment provides enough stream inflow to sustain SWBs. This

Table 1. Hypothetically represented flood and drought transformations by means of S of specified diameter and their relation with normalized stream flow discharge values.

Stream flow in normalized scale	Diameter of S in pixels	Process	Stream flow in normalized scale	Diameter of S in pixels	Process
1	10	Flood	0.4	6	Drought
0.9	9	Flood	0.3	7	Drought
0.8	8	Flood	0.2	8	Drought
0.7	7	Flood	0.1	9	Drought
0.6	6	Flood	0.0	10	Drought
0.5	0	No Process	–	–	–

Table 2. Morphological transformations due to stream flow discharge template derived from varied normalized stream flow discharge values.

N	Stream flow discharge	Notation	Environmental phase	N	Stream flow discharge	Notation	Environmental phase
15	1.0000	$M \oplus S_{15}$		1	0.4666	$M \ominus S_1$	
14	0.9666	$M \oplus S_{14}$		2	0.4333	$M \ominus S_2$	
13	0.9333	$M \oplus S_{13}$		3	0.4000	$M \ominus S_3$	
12	0.9000	$M \oplus S_{12}$		4	0.3666	$M \ominus S_4$	
11	0.8666	$M \oplus S_{11}$		5	0.2222	$M \ominus S_5$	D
10	0.8333	$M \oplus S_{10}$	F	6	0.3000	$M \ominus S_3$	R
9	0.8000	$M \oplus S_9$	L	7	0.2666	$M \ominus S_2$	O
8	0.7666	$M \oplus S_8$	O	8	0.2333	$M \ominus S_8$	U
7	0.7333	$M \oplus S_7$	O	9	0.2000	$M \ominus S_9$	G
6	0.7000	$M \oplus S_6$	D	10	0.1666	$M \ominus S_{10}$	H
5	0.6666	$M \oplus S_5$		11	0.1333	$M \ominus S_{11}$	T
4	0.6333	$M \oplus S_4$		12	0.1000	$M \ominus S_{12}$	
3	0.6000	$M \oplus S_3$		13	0.0666	$M \ominus S_{13}$	
2	0.5666	$M \oplus S_2$		14	0.0333	$M \ominus S_{14}$	
1	0.5333	$M \oplus S_1$		15	0.0000	$M \ominus S_{15}$	
0	0.5000	$M \ominus S_0$	Stable				

facilitates visualization of various possible spatio-temporal organizations of SWBs (Fig. 5). For example, the interplay between numerically simulated stream flow discharge and its impact on the spatially distributed SWBs is assumed for a case when λ=3.99 as the amount of stream flow discharge in succeeding times is oscillating chaotically between increasing and decreasing to dissimilar degrees. It means that SWBs are undergoing C-FD transformation, in which the flood followed by drought are not of the same degree. If we see the whole process in a reverse way, then the SWBs undergo C-DF to varied degrees. For further changes in λ, one can visualize the other discrete spatio-temporal patterns of SWBs. In a sense, the SWBs' morphological dynamics are a coupled system that depends on dynamics of stream flow discharge. While considering the MSD as the basis, a heuristically true argument is that the reduction in stream flow discharge that is capable of vanishing the water bodies of all sizes may be equivalent to the amount of stream flow discharge that is capable of making multiple water bodies merge together. In support of this argument, number of drought cycles due to S required to vanish the SWBs in a floodplain basin is equivalent to the number of flood cycles due to S required to merge SWBs. The amount of stream flow discharge much lesser than (or) much greater than MSD, respectively, indicates the presence of drought and floods. By presuming A_{t+1} much lesser than MSD, i.e. 0, and A_{t+1} much greater than MSD, i.e. 1, various stream flow discharge behavioral patterns are simulated.

To link the stream flow discharge data simulated under varied λs, with the degree of either flood or drought, we adapt the procedure by considering a relationship between *SOCCNM* and *FDN* (e.g. Fig. 4b). This relationship explains the time required by two neighboring SWBs to merge. For the present case, *FDN* and *SOCCNM* are shown in blue and cyan colors for SWBs (Fig. 5). Performing Eqs. (4)–(7) up to Nth cycle yields the last level of subsets of *SOCCNM* and *FDN*. It is presumed that S_N to attain FDN_N (M) is equivalent to S_N to attain SOCCNM_N (M). This S_N is considered as the template in matrix form (e.g. Fig. 1e) to simulate either complete flooding or drought.

The S_N is related with the largest stream flow discharge value that is able to merge the neighboring water bodies.

Further, this S_N is taken as the basis to decide the other possible templates of various smaller sizes, correspondingly to relate with other stream flow discharge values. For instance, the maximum distance that is estimated from the Nth level subsets of $FDN_N(M)$ and $SOCCNM_N(M)$ of water bodies is $S_N \oplus S_N$=1 (stream flow discharge in normalized scale) and S_N=0.5 (stream flow discharge in normalized scale) that makes water bodies attain their full capacity. Similarly, when there is absolutely no stream flow discharge, such an aspect is linked to the minimum value in the time series of simulated stream flow discharge in the normalized scale, i.e. 0. The water bodies at stability state attain their full capacity filled due to the presence of consistent MSD (Table 1). With an environmental parameter (λ) value of 2, all the SWBs attain stability as there would be no change in the simulated stream flow discharges across discrete time intervals. When the pattern of stream flow discharge is unusual, the climatically sensitive SWBs behave differently. For the present case, the MSD is assumed as 0.5 that makes all water bodies attain their full level. This explains the impact of variations in the stream flow discharge pattern on the spatial organization of the water bodies that are assumed to be at stable state under the availability of stream flow discharge of 0.5.

A stream flow discharge less than MSD makes the SWBs contract, while a stream flow discharge greater than MSD makes the SWBs expand. By means of this template, MSD (i.e. 0.5 in normalized scale) and stream flow discharge value simulated from logistic equation, we impose an appropriate morphological transformation. To determine the involved morphological transformation, we check the stream flow discharge values at discrete time intervals with reference to 0.5 (i.e. MSD). These relationships are depicted as.

$$\begin{aligned} &\text{If} \quad A_{t+1} \quad > 0.5, \quad \text{then} \quad M \oplus S_N \\ &\text{If} \quad A_{t+1} \quad < 0.5, \quad \text{then} \quad M \ominus S_N \\ &\text{If} \quad A_{t+1} \quad = 0.5, \quad \text{then} \quad M \oplus S_0. \end{aligned} \tag{8}$$

In other words, maximum level of flood that merges all the water bodies under the availability of stream flow discharge that is much higher than the MSD is expressed with a morphological relationship as follows.

$$[FDN\,(M) \oplus S_N \oplus S_N] = [M \oplus S_N]\,, \tag{9}$$

where S_N, and S_0 , are the sizes of templates that are equated with normalized stream flow discharge values, respectively, at 1 and 0. Similarly, the stream flow discharges that keep the water bodies at stable levels and vanish, respectively, are morphologically related as

$$[FDN\,(M) \oplus S_N] = [M \oplus S_0]\,, \tag{10}$$

$$[M \ominus S_N] = [FDN\,(M) \oplus S_0]\,. \tag{11}$$

4 Results

For SWBs' case, S_N is derived as the template with the radius of 15 pixels. The template with a radius of 15 pixels

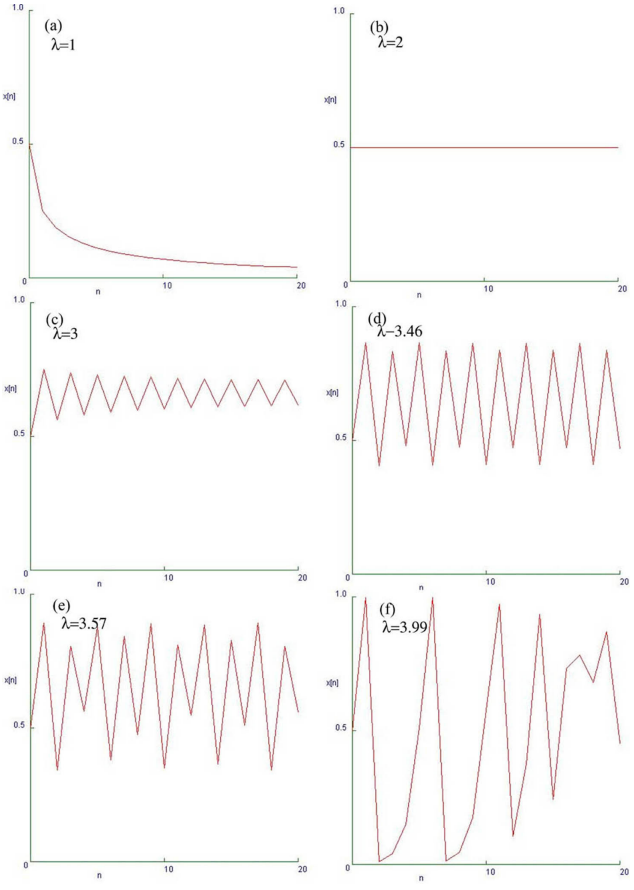

Fig. 7. Streamflow discharge behavioral pattern at different environmental parameters. **(a)–(f)** λ=1, 2, 3, 3.46, 3.57 and 3.99.

is required to vanish the water bodies of various sizes in the section under the drought transformation. Hence to relate the template with a radius of 15 pixels to the normalized stream flow discharge values, 0.5 is divided by 15, which yields each cycle of either drought or flood transformation with the interval of 0.03333. Table 2 depicts these details with the involved morphological processes at respective stream flow discharge values. The higher the number of cycles that a section containing the water bodies requires to establish either *FDN* or *SOCCNM*, the closer the comparison with the values in normalized scale.

Variations in stream flow discharges are due to several factors that include rainfall pattern and landscape topological organization. Time series of such fluctuating stream flow discharges is simulated according to the first order nonlinear difference equation as observed stream flow records are insufficient. These simulated data are considered to study how the boundaries of the SWBs are modified. The morphological behaviors of SWBs under varied simulated stream flow discharge behavioral pattern, by considering initial stream flow discharge A_0=0.5 for all the cases and $\lambda \in$ (1, 4), are simulated. This phenomenon is better explained through the logistic map (Fig. 7). Various types of morphological behaviors of SWBs include attracting to initial conditions, stable,

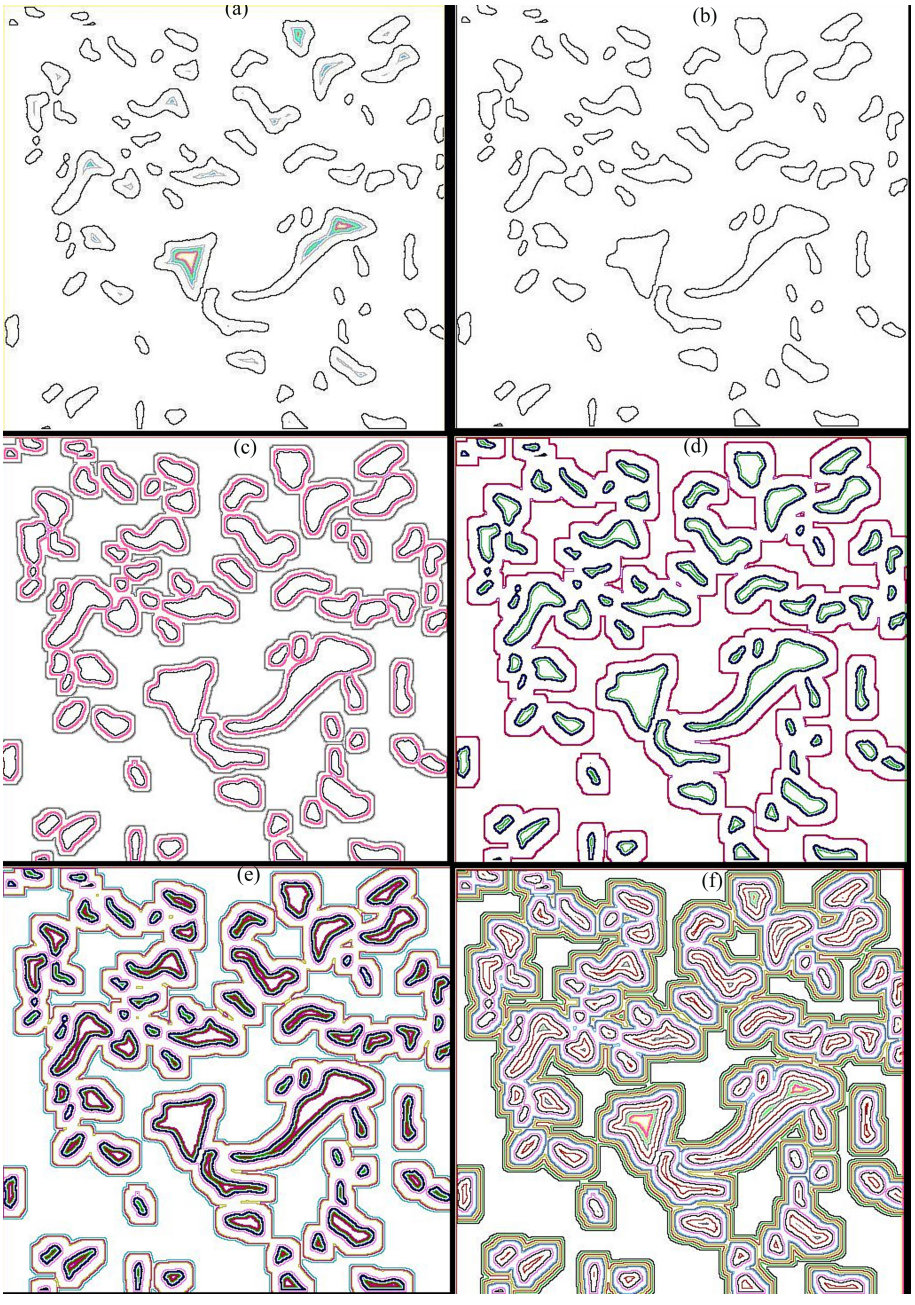

Fig. 8. Spatio-temporal organization of the surface water bodies under the influence of various streamflow discharge behavioral patterns at the environmental parameters at **(a)–(f)** λ=1, 2, 3, 3.46, 3.57, and 3.99 are shown upto 20 time steps. In all the cases, the considered initial MSD, A_0=0.5 (in normalized scale) is considered under the assumption that the water bodies attain their full capacity. It is illustrated only for the overlaid outlines of water bodies at respective time-steps with various λs.

periodically changing and chaotically changing are simulated (Figs. 8a–8f). The water bodies' boundaries (B_M) at the next time period is defined as a function of that of the preceding time period and given as $B_{M_{t+1}}=f(B_{M_t})$, where B_{M_t} is $[M_t-(M_t \ominus S_1)]$. The union of boundaries of the dynamically changing SWBs, which are superimposed patterns, is termed as attractor describing the morphological dynamics of SWBs under varied stream flow discharge dynamics. The attractor of SWBs space-time morphological dynamics is defined as:

$$\bigcup_{t=0}^{n}[B_{M_t}], \tag{12}$$

where M_0 is a section consisting of water bodies during the presence of mean stream flow discharge (MSD). The impact of varied stream flow discharge dynamics, simulated numerically via first order nonlinear difference equation, on the

Table 3. Fractal dimensions of SWBs attractors.

Environmental parameter, λ	SWB
1	1.58
2	1.53
3	1.78
3.46	1.76
3.57	1.84
3.99	1.90

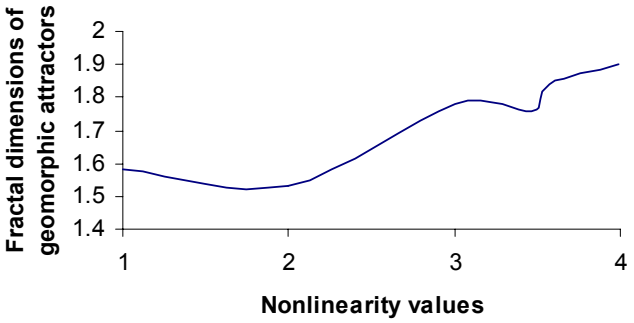

Fig. 9. Relationship between λ and fractal dimension of geomorphic attractors.

SWBs is visualized by synchronizing with appropriate degrees of contraction and expansion (Fig. 8).

The computed fractal dimensions of the spatio-temporal patterns of SWBs that are simulated by considering the time series of stream flow discharge simulated at λ=1, 2, 3, 3.46, 3.57, and 3.99, respectively, are 1.58, 1.52, 1.78, 1.72, 1.84, and 1.90 (Fig. 9 and Table 3). It is apparent from the fractal dimensions of these attractors that, the higher the fractal dimension the higher is the randomness in the morphological behavior. When λ is 1 and 3, the spatio-temporal patterns of SWBs exist (or) completely occupy the region within the SWBs at is attained under the availability of MSD. Hence, the fractal dimensions are higher than that of the succeeding threshold control parameters, e.g. λ=2 and 3.46. The spatio-temporal patterns, which have aroused under the influence of λ values of 2 and 3.46 are, respectively, one or two patterns. Hence the fractal dimensions are lesser than their preceding λ values. The higher the fractal dimension, the greater is the difficulty in predicting the behavior. The rises and falls of the levels of water bodies lead to a dynamic sequence of adjustment throughout the year.

5 Conclusions

In this paper, we provide a simple scheme to relate time series of stream flow discharge with templates to simulate the various possible morphological dynamics of small water bodies in two-dimensional space. We employ mathematical morphological transformations to show such a relationship under certain theoretical assumptions. These assumptions are primarily based on a postulate that enlargements and contractions of SWBs are due to fluctuations in the stream flow discharge pattern. In the present investigation, the studies on spatio-temporal organization of randomly situated SWBs are carried out in discrete space under the influence of various stream flow discharge behaviors.

Acknowledgements. Comments and suggestions provided by B. Sivakumar, F. Laio and an anonymous reviewer are gratefully acknowledged.

Edited by: B. Sivakumar
Reviewed by: F. Laio and another referee

References

Beauvais, A. and Dubois, J.: Attractor properties of a river discharge dynamical system, Eos Transations AGU, 73, 46, F234, 1995.

Chockalingam, L., Sagar, B. S. D.: Automatic generation of subwatershed map from Digital Elevation Model: a morphological approach, International Journal of Pattern Recognition and Artificial Intelligence, 17, 2, 269–274, 2003.

Harris, A. R.: Time series remote sensing of a climatically sensitive lake, Rem. Sen. Env., 50, 83–94, 1994.

Jayawardena, A. W. and Lai, F.: Analysis and prediction of chaos in rainfall and streamflow time series, J. Hydr., 153, 23–52, 1994.

Matheron G.: Random sets and integrated geometry, Wiley, New York, 1975.

May, R. M.: Simple mathematical models with very complicated dynamics, Nature, 261, 459–467, 1976.

Pasternack, G. B.: Does the river run wild? Assessing chaos in hydrological systems, Adv. Water Resour., 23, 253–260, 1999.

Sagar, B. S. D. and Rao, B. S. P.: Fractal relation on perimeter to the water body area, Current Science, 68, 5, 1129–1130, 1995.

Sagar, B. S. D., Gandhi, G., and Rao, B. S. P.: Applications of mathematical morphology on water body studies, Int. J. Rem. Sens., 16, 8, 1495–1502, 1995a.

Sagar, B. S. D., Venu, M., and Rao, B. S. P.: Distributions of surface water bodies, Int. J. Rem. Sens., 16, 16, 3059–3067, 1995b.

Sagar, B. S. D.: Fractal relations of a morphological skeleton, Chaos, Solitons and Fractals, 7, 5, 1871–1879, 1996.

Sagar, B. S. D., Omoregie, C., and Rao, B. S. P.: Morphometric relations of fractal-skeletal based channel network model, Discrete Dynamics in Nature and Society, 2, 2, 77–92, 1998.

Sagar, B. S. D., Venu, M., Gandhi, G., and Srinivas, D.: Morphological description and interrelationship between force and structure: a scope to geomorphic evolution process modelling, Int. J. Rem. Sens., 19, 7, 1341–1358, 1998.

Sagar, B. S. D., Venu, M., and Murthy, K. S. R.: Do skeletal network derived from water bodies follow Horton's laws?, Mathem. Geol., 31, 2, 143–154, 1999.

Sagar, B. S. D.: Estimation of number-area-frequency dimensions of surface water bodies, In. J. Rem. Sens., 20, 13, 2491–2496, 1999.

Sagar, B. S. D.: Fractal relation of medial axis length to the water body area, Discrete Dynamics in Nature and Society, 4, 1, 97, 2000.

Sagar, B. S. D. and Murthy, K. S. R.: Generation of fractal landscape using nonlinear mathematical morphological transformations, Fractals, 8, 1, 267–272, 2000.

Sagar, B. S. D., Venu, M., and Srinivas, D.: Morphological operators to extract channel networks from Digital Elevation Models, Int. J. Rem. Sens., 21, 1, 21–30, 2000.

Sagar, B. S. D., Srinivas, D., and Rao, B. S. P.: Fractal skeletal based channel networks in a triangular initiator basin, Fractals, 9, 4, 429–437, 2001.

Sagar, B. S. D.: Generation of self organized critical connectivity network map (SOCCNM) of randomly situated surface water bodies, Letters to Editor, Discrete Dynamics in Nature and Society, 6, 1, 225–228, 2001.

Sagar, B. S. D.: Hypothetical laws while dealing with effect by cause in discrete space, Letter to the Editor, Discrete Dynamics in Nature and Society, 6, 1, 67–68, 2001.

Sagar, B. S. D., Murthy, M. B. R., Rao, C. B., and Raj, B.: Morphological approach to extract ridge-valley connectivity networks from Digital Elevation Models (DEMs), Int. J. Rem. Sens., 24, 1, 573–581, 2003.

Sagar, B. S. D. and Tien, T. L.: Allometric power-law relationships in a Hortonian Fractal DEM, Geophys. Res. Lett., 31, 2, L06501, 2004.

Sagar, B. S. D. and Chockalingam, L.: Fractal dimension of non-network space of a catchment basin, Geophys. Res. Lett., 31, 6, L12502, 2004.

Savard, C. S.: Correlation integral analysis of South Twin River streamflow, central Nevada: preliminary application of chaos theory, Eos Transaction AGU, 71, 43, 1341, 1990.

Savard, C. S.: Looking for chaos in streamflow discharge derivative data, Eos Transactions AGU, 73, 14, 50, 1992.

Serra J.: Image analysis and mathematical morphology, Academic Press, New York, 1982.

Sivakumar, B.: Chaos theory in geophysics: past, present and future, Chaos Solitons and Fractals, 19, 2, 441–462, 2004.

Tsonis, A. A., Triantafyllou, G. N., and Elsner, J. B.: Searching for determinism in observed data: a review of the issue involved, Non. Proc. Geophys., 1, 12–25, 1994,
SRef-ID: 1607-7946/npg/1994-1-12.